JPE 14-1-15

http://dx.doi.org/10.6113/JPE.2014.14.1.143
ISSN(Print): 1598-2092 / ISSN(Online): 2093-4718

Generalized Stability Criterion for Multi-module Distributed DC System

Fangcheng Liu*, Jinjun Liu†, Haodong Zhang*, and Danhong Xue*

*†State Key Laboratory of Electrical Insulation and Power Equipment, School of Electrical Engineering, Xi'an Jiaotong University, Xi'an, China

Abstract

The stability issues of a multi-module distributed DC power system without current-sharing loop are analyzed in this study. The physical understanding of the terminal characteristics of each sub-module is focused on. All the modules are divided into two groups based on the different terminal property types, namely, impedance (Z) and admittance (Y) types. The equivalent circuits of each group are established to analyze the stability issues, and the mathematical equations of the equivalent circuits are derived. A generalized criterion for multi-module distributed systems is proposed based on the stability criterion in a cascade system. The proposed criterion is independent of the power flow direction.

Keywords: Multi-module distributed system, Stability criterion, Terminal characteristics

I. INTRODUCTION

Compared with traditional power conversion systems, a multi-module distributed system has the following advantages: 1) it provides the possibility of coordinating several sources and loads; 2) the power and voltage rating can easily be increased by connecting different modules in cascade or parallel; and 3) production and maintenance are easier because of the standardized design. Multi-module distributed systems have been widely adopted in practical applications because of these benefits.

However, the dynamic characteristics of each sub-module in the system are different; thus, the interaction among different sub-modules limits the performance of the total system. Although each sub-module is stable in stand-alone mode, the total system may be unstable because of the interaction.

The stability issues of multi-module systems have been discussed in several studies [1–4]. Following the impedance-based stability criterion in the cascade DC system [5], the multi-module system is divided into two groups: source and load groups. The interaction between the two groups is considered. The equivalent output impedance of the source group and the equivalent input impedance of the load group are utilized to evaluate the stability of the system. The validity of this criterion has been proven in a system where all source modules are utilized to regulate the DC bus voltage [4]. However, the validity of this criterion cannot be guaranteed in a system where the control objectives of some source modules are not DC bus voltages. A four-module system is shown in Fig. 1. Only one source converter is controlled to regulate the DC bus voltage, and another source converter is controlled to realize maximum power point tracking. This four-module system is a typical system in renewable energy applications and is quite different from the system studied in existing research on stability analysis.

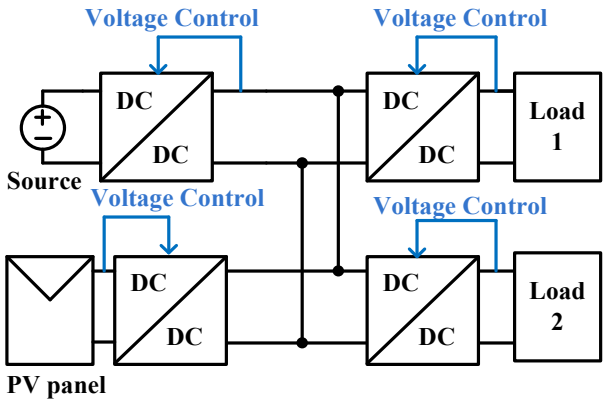

Fig. 1. Four-module distributed system.

The stability issues of cascade systems no longer rely on

Manuscript received Jul. 19, 2013; revised Nov. 4, 2013
Recommended for publication by Associate Editor Jun-Keun Ji.
†Corresponding Author: jjliu@mail.xjtu.edu.cn
Tel: +86-29-82668919, Xi'an Jiaotong University
*State Key Laboratory of Electrical Insulation and Power Equipment, School of Electrical Engineering, Xi'an Jiaotong University, China

the distinction between the source and load [6]-[8]. Instead, the terminal property of each sub-module becomes the key point in stability analysis. This study provides a new concept to analyze the stability issues of multi-module systems according to the terminal property of each sub-module.

This study aims to analyze the stability issues of multi-module distributed systems by 1) defining the different terminal characteristics of each sub-module, 2) recognizing that the stability criterion of multi-module systems does not depend on the power flow direction, and 3) developing a new criterion for multi-module distributed systems.

The distinction of the terminal characteristics of a single sub-module is analyzed in Section II. The measurement of terminal impedance and admittance is briefly introduced in Section III. The total system is divided into two equivalent groups (Z and Y) according to the terminal property of each sub-module. The equivalent circuit of the total system is drawn, and the stability issues are analyzed in Section IV. Some basic considerations for stability enhancement are presented in Section V based on the proposed stability criterion. The experimental findings are presented in Section VI.

II. TERMINAL CHARACTERISTICS OF SUB-MODULES

Only the distributed system without current-sharing loop (CSL) is considered in this study. Otherwise, the effective structure of the total system with CSL will differ if CSL varies. The influence of a detailed controller design should be considered in assessing the stability of the total system with CSL. The general stability criterion is unavailable because the effective structure of the total system with CSL is not fixed [9]. However, no interaction occurs in the control part among different sub-modules in the system without CSL, and only the electrical interaction in the power stage affects stability. Therefore, the stability issues of the distributed system without CSL are caused only by the electrical interaction among different sub-modules in the power stage.

The external behavior of each sub-module is provided more attention than its internal loop stability in the analysis of the electrical interaction in the power stage. In such cases, the terminal impedance/admittance-based approach is advantageous and effective because it avoids the detailed model of each module, especially when the detailed design information of individual modules is unavailable.

In a DC system, only two variables exist at a common terminal: current and voltage. Hence, the relationship between terminal current and voltage describes the terminal characteristics of each module. The terminal impedance or admittance of the converter is the linearized model of terminal behavior around a certain operating point. When the terminal property of the active module is considered, the terminal characteristics depend not only on the power stage but also on the controller as shown in Fig. 2.

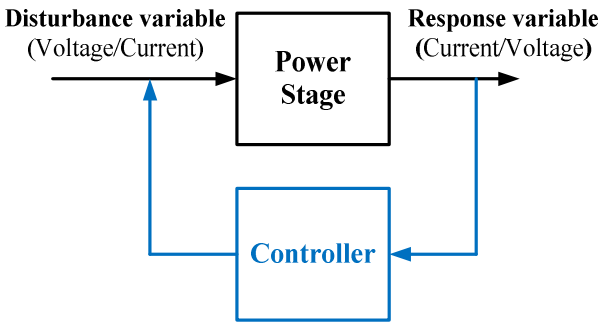

Fig. 2. Structure of the active module.

The disturbance variable should be distinguished from the response variable in the controller design. The distinction relates to the available external source in the primary design. The different sets characterize only one main type of converter and are not interchangeable [10]. Transfer function T_1 from the disturbance variable to the response variable should be stable in the controller design. Only the right half plane poles (RHP) in the transfer function affect the stability of the sub-module [11]. Therefore, no RHP is allowed in closed-loop transfer function T_1, and the number of right half plane zeros (RHZ) in T_1 is not required in the controller design. Conversely, the stability of equivalent transfer function T_2 (equal to $1/T_1$) from the response variable to the disturbance variable is not guaranteed. Thus, the active module is a non-minimum phase system in some cases. In addition, T_1 follows the signal flow path and is organized as the signal process from input to output, whereas T_2 does not. Therefore, only one type of transfer function T_1 in terminal characteristics is physically reasonable in primary converter design because no RHP is included. The other type of transfer function T_2 is merely an equivalent mathematical expression, and its physical meaning is not reasonable because of the possible existence of RHP in T_2 (equal to the possible RHZ in T_1).

In normal cases, only one ideal source is appropriate at the input or output terminal of the active converter because of the limitation in topology design. For example, if a capacitor is connected in parallel with an ideal voltage source, the effect of the capacitor is attenuated by the voltage source, and the capacitor may be damaged because of the overcurrent when the voltage source changes abruptly. Therefore, the capacitor should avoid direct parallel connection with the ideal voltage source. For a similar reason, the inductor should avoid direct serial connection with the ideal current source. An active converter can be classified into two groups, namely, current-fed (CF) and voltage-fed (VF) converters, according to the available source at the common terminal.

In a VF converter, terminal voltage is regarded as the disturbance variable, whereas terminal current is regarded as the response variable [12], [13]. Thus, the terminal

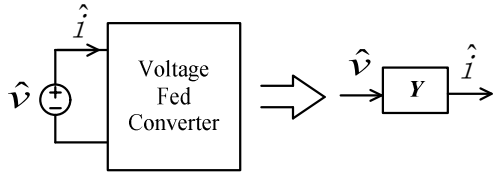

Fig. 3. Terminal characteristic of a VF converter.

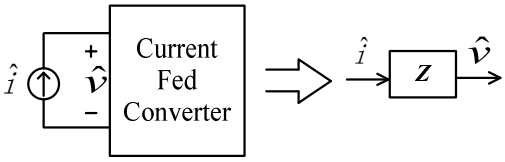

Fig. 4. Terminal characteristic of a CF converter.

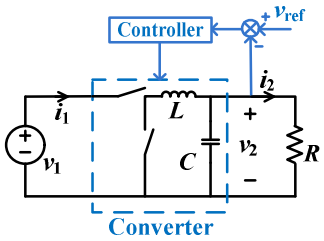

Fig. 5. Example of constant power load.

characteristic is equivalent to admittance (Y) as shown in Fig. 3. No RHP is allowed in terminal admittance because the VF converter should be stable in standalone mode.

CF converters are still used in practical applications as discussed in [6] and [14]. Terminal current should be regarded as the disturbance variable, and terminal voltage should be regarded as the response variable in a CF converter. The terminal characteristic of a CF converter is equivalent to impedance (Z) as shown in Fig. 4.

In practical applications, RHZ may be induced by a complicated control design or the intrinsic nature of some systems. The most typical example of a single module with RHZ is the constant power load (CPL) application. When a converter tightly strictly regulates its output, it behaves as a CPL at the input terminals. A simple example of CPL is shown in Fig. 5. The input power equals the output power because the power loss of the converter can be neglected. CPL indicates that steady-state input power is constant and instantaneous input power may not be constant.

The problem of CPLs is that they exhibit negative incremental resistance, which may cause negative impedance instability in the system, as shown in Fig. 6 [15], [16].

If a small increment exists in v_1, input current i_1 will decrease to maintain the input power constant as shown in Fig. 7. Therefore, only one variable of Δv_1 and Δi_1 is positive, and the other one must be negative. If a resistor is utilized to model the relationship between Δv_1 and Δi_1, the following can be derived.

$$R = \frac{\Delta v_1}{\Delta i_1} < 0 \tag{1}$$

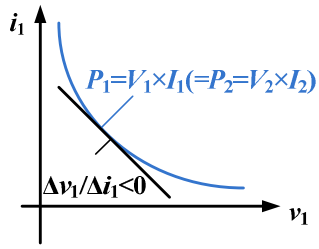

Fig. 6. Negative impedance behavior of constant power load.

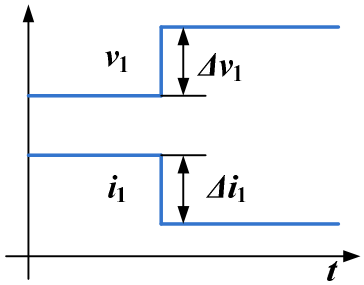

Fig. 7. Waveforms of constant power load.

Negative incremental impedance can be characterized by RHZ in the small signal transfer function [17, 18]. However, no RHP exists in the transfer function of terminal characteristics because the system is stable.

III. Terminal Impedance/Admittance Measurement

The type of terminal characteristics (impedance or admittance) is easy to obtain even if the detailed model of each module is unknown because the type of available external source is always known. Detailed magnitude and phase information can be easily measured by a commercial network analyzer. The merits of a network analyzer are as follows: 1) it can provide an excitation signal of variable frequency and 2) it can automatically calculate the real and imaginary parts of a measured variable. Moreover, several additional devices are required to conduct measurements. First, the terminal impedance/admittance of the converter is a small signal model. Therefore, an appropriate external source and load are required to make the converter work at a certain operating point. Second, the output power of the network analyzer is limited; thus, suitable amplifier circuits are necessary to match the injected perturbation and the operating point. Third, suitable sampling circuits are required to measure the desired variables. Some typical measurement setups are presented in [19] to [21].

The measurement of the VF converter is presented as an example in Fig. 8. Voltage source v_1 is added to make the converter work at the operating point. Terminal voltage is regarded as the disturbance variable; thus, an amplifier circuit is used to inject a disturbance voltage of suitable amplitude

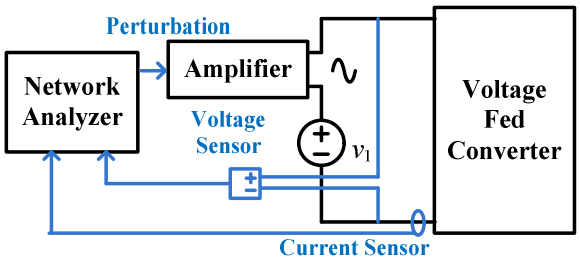

Fig. 8. Measurement of the terminal admittance of the VF converter.

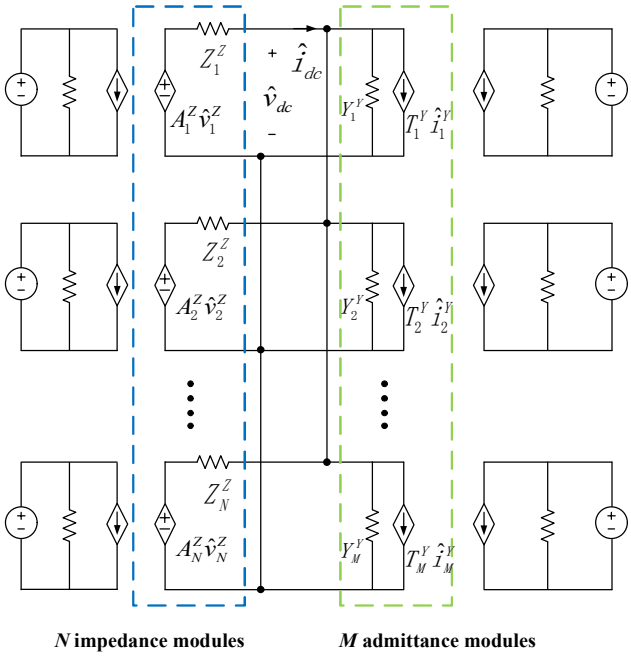

Fig. 9. Multi-module distributed system.

because the output power of the network analyzer is limited. The network analyzer can compute the terminal admittance based on the measured voltage and current by calculating the ratio of the measured current to the measured voltage in the frequency domain.

IV. Equivalent Circuit and Stability Analysis

The equivalent circuit of each module can easily be drawn according to basic circuit theory when the type of terminal property is fixed [22]. The terminal property of a common bus terminal is more attractive in stability analysis; thus, only the characteristics of the common bus terminal of each module are concerned.

The Thevenin equivalent circuit is utilized to model the terminal characteristics of the Z-type module, whereas the Y-type module is represented by the Norton equivalent circuit in general cases. This set allows for a clear subsequent analysis. If the Norton equivalent circuit is used for the Z module where terminal voltage is regulated tightly, an infinite

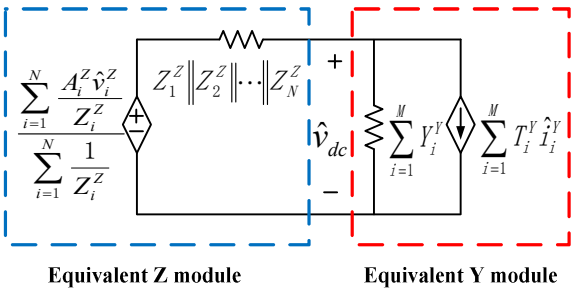

Fig. 10. Equivalent circuit of the multi-module system.

current source is required because terminal impedance is almost zero at 0 Hz. An infinite current source is unacceptable in both practical applications and theoretical analyses.

A multi-module system without CSL is shown in Fig. 9. All the Z-type modules are represented by the Thevenin equivalent circuit, and all the Y-type modules are represented by the Norton equivalent circuit.

The simplified equivalent circuit of the total system is shown in Fig. 10. All the Z-type modules are replaced by an equivalent Z-type module, and all the Y-type modules are replaced by an equivalent Y-type module. This equivalent circuit is similar to the circuit shown in the stability analysis of cascade systems [23].

The mathematical expression of DC bus voltage can then be derived as

$$\hat{v}_{dc}=\frac{\sum_{i=1}^{N}\frac{A_i^Z\hat{v}_i^Z}{Z_i^Z}\cdot(Z_1^Z\|Z_2^Z\|\cdots\|Z_N^Z)-(Z_1^Z\|Z_2^Z\|\cdots\|Z_N^Z)\cdot\sum_{i=1}^{M}T_i^Y\hat{i}_i^Y}{1+(Z_1^Z\|Z_2^Z\|\cdots\|Z_N^Z)\cdot\sum_{i=1}^{M}Y_i^Y} \quad (2)$$

Given that each sub-module is stable in stand-alone mode, no RHP should exist in the numerator in (2). The stability of the total system then depends on the number of RHZ in the denominator in (2).

The detailed models of some modules are sometimes unknown in practical applications. In this case, the mathematical transfer function cannot be derived. However, the terminal characteristics of these modules can be estimated according to the data measured by the network analyzer. When the measured data are analyzed, graphic stability analysis methods, such as the Nyquist stability criterion, are suitable.

When the Nyquist stability criterion is applied to (2), system stability can be assessed from T_m in (3).

$$T_m=(Z_1^Z\|Z_2^Z\|\cdots\|Z_N^Z)\cdot\sum_{i=1}^{M}Y_i^Y \quad (3)$$

The basic equation of the Nyquist stability criterion is shown in (4). When the number of times open-loop frequency response T_m encircles point (-1, 0) in counter-clockwise direction equals the number of RHP in T_m, the system is stable [11].

$$N_{Tm} = RHZ(1 + T_m) - RHP(T_m) \quad (4)$$

where N_{Tm} is the number of clockwise encirclements of the critical point (-1, 0), $RHZ(1+T_m)$ is the number of RHZ in $1+T_m$, and $RHP(T_m)$ is the number of RHP in T_m.

The number of RHZ in $1+T_m$ is of concern because it directly influences the stability of the total system.

N_{Tm} can be drawn based on the measured data. Therefore, the number of RHPs in T_m should be estimated before the Nyquist criterion is applied to T_m.

As shown in (3), T_m has two parts, namely, the equivalent impedance of all the Z-type modules ($Z_{eq} = Z_1^Z \| Z_2^Z \| \cdots \| Z_N^Z$) and the equivalent admittance of all the Y-type modules ($Y_{eq} = \sum_{i=1}^{M} Y_i^Y$). Given that all the modules must be stable in stand-alone mode, no RHP exists in the equivalent admittance of all Y-type modules. Hence, only the number of RHP in the equivalent impedance of all Z-type modules should be estimated.

Z_{eq} can then be expressed as (5).

$$Z_{eq} = Z_1^Z \| Z_2^Z \| \cdots \| Z_N^Z = \frac{\prod_{i=1}^{N} Z_i^Z}{\sum_{i}^{N} (\frac{1}{Z_i^Z} \cdot \prod_{j=1}^{N} Z_j^Z)} \quad (5)$$

Given the stability requirement for the sub-module in stand-alone mode, no RHP exists in the numerator. Therefore, only the number of RHZ in the denominator should be estimated.

Similarly, the Nyquist criterion is applied to the denominator of Z_{eq} to assess the number of RHZ in $\sum_{i}^{n} \frac{1}{Z_i} \cdot \prod_{j=1}^{n} Z_j$.

$$N_{\sum_i^N (\frac{1}{Z_i^Z} \cdot \prod_{j=1}^{N} Z_j^Z)} = RHZ(\sum_{i}^{N} (\frac{1}{Z_i^Z} \cdot \prod_{j=1}^{N} Z_j^Z)) - RHP(\sum_{i}^{N} (\frac{1}{Z_i^Z} \cdot \prod_{j=1}^{N} Z_j^Z)) \quad (6)$$

The definitions of each item in (6) are similar to those in (4). However, the critical point is changed to (0, 0) because of the mathematical application. The number of RHP in $\sum_{i}^{n} \frac{1}{Z_i} \cdot \prod_{j=1}^{n} Z_j$ is also zero. Therefore, (6) can be simplified to (7).

$$N_{\sum_i^N (\frac{1}{Z_i^Z} \cdot \prod_{j=1}^{N} Z_j^Z)} = RHZ(\sum_{i}^{N} (\frac{1}{Z_i^Z} \cdot \prod_{j=1}^{N} Z_j^Z)) \quad (7)$$

Based on the analysis above, a two-step stability criterion is proposed as follows.

1) The trajectory of $\sum_{i}^{n} \frac{1}{Z_i} \cdot \prod_{j=1}^{n} Z_j$ (the denominator of $Z_1^Z \| Z_2^Z \| \cdots \| Z_N^Z$) is drawn on s-plane. The number of times the trajectory encircles point (0,0) in clockwise direction is equal to the number of RHP in Z_{eq}.

2) The trajectory of $Z_{eq} \cdot Y_{eq}$ is drawn on s-plane. If the number of times the trajectory encircles point (-1, 0) in a counter-clockwise direction equals the number of RHP in Z_{eq}, then the system is stable; otherwise, the system is unstable.

The first step can be explained as the assessment of the interaction among all the Z-type modules. If only one Z-type module exists in the system, no interaction occurs and the denominator of Equation (5) is 1. The first step can then be neglected, and only the second step is required. The second step is implemented to assess the interaction between the equivalent Z module and equivalent Y module.

The proposed criterion is clearly independent of the power flow direction. However, the detailed information of the small signal terminal characteristics of the sub-module changes when the operating point changes. Therefore, the stability of the distributed multi-module system should be reassessed when the operating point changes.

V. Stability Enhancement

The stability issues of a distributed multi-module system are caused by the electrical interaction among different sub-modules in the power stage. Therefore, the stability of the total system can be enhanced by weakening the electrical interaction. According to the proposed stability criterion, two types of electrical interaction exist in the system: 1) the interaction among all the Z-type modules and 2) the interaction between the equivalent Z module (Z_{eq}) and equivalent Y module (Y_{eq}).

A. Interaction among the Z-type Modules

If the system instability is caused by the interaction among all the Z-type modules, stability can be improved by decreasing the impedance of some modules or using an additional DC bus conditioner [24].

When the terminal impedance of one module is decreased, the dynamic response of this module becomes fast. If the impedance of module i is much smaller than that of the other modules ($Z_i << Z_1, Z_2, \cdots, Z_n$), module i is a more ideal voltage source than others, and the dynamic characteristics of the other modules can be neglected. Therefore, the interaction among all the Z-type modules can be neglected. The equivalent impedance of all the Z-type modules is approximately equal to the impedance of module i (Z_i) in this case as (8).

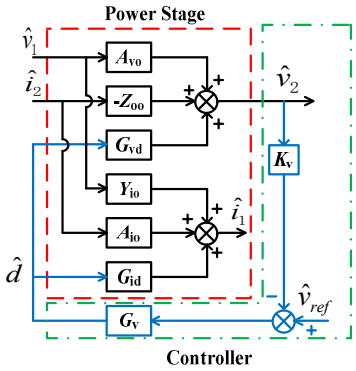

Fig. 11. Small signal model of constant power load in Fig. 5.

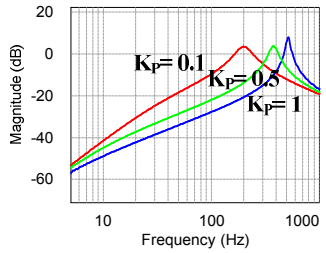

Fig. 12. Terminal impedance Z_2 under different K_P.

$$Z_{eq} = Z_1 \,||\, Z_2 \,||\, \cdots \,||\, Z_n \approx Z_i \tag{8}$$

Given that each sub-module is stable in stand-alone mode, Z_i and Z_{eq} must also be stable. Therefore, the interaction among all the Z-type modules is weakened and stability is enhanced.

The methods utilized to decrease terminal impedance depend on the detailed inner structure of the converters because the detailed models of the converters are different [25–27]. For example, the small signal model of the CPL converter in Fig. 5 is shown in Fig. 11.

Output impedance Z_2 can be expressed as (9).

$$Z_2 = \frac{-Z_{oo}}{1 + G_v K_v G_{vd}} \tag{9}$$

Z_2 decreases when the modulus of voltage loop regulator G_v increases. A simple PSIM simulation result shows that the low-frequency part of Z_2 decreases when the proportional coefficient K_P (G_v is a proportional-integral regulator) increases in Fig. 12. The simulation parameters are L = 1 mH, C = 1.5 mF, R = 1 Ω, v_1 = 30 V, v_{ref} = 12 V, and K_I = 30.

Terminal impedance can also be decreased by changing other parameters in the power stage or controller. The changes in the parameters will also change the total performance of the converter; thus, the adjustment should consider the influence on different aspects rather than the stability issues.

The interaction among all the Z-type modules can also be weakened by a DC bus conditioner. When the impedance of DC bus conditioner Z_{n+1} is much smaller than that of other modules (Z_{n+1}<<Z_1, Z_2,⋯, Z_n), most of the disturbance current is absorbed by the bus conditioner and the dynamic characteristics of the other modules can be neglected. Therefore, the interaction among all the Z-type modules can be neglected.

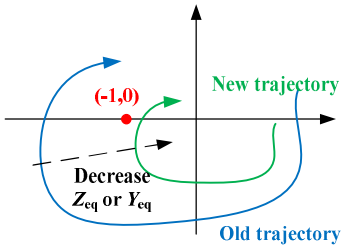

Fig. 13. Stability enhancement by decreasing Z_{eq} or Y_{eq}.

B. *Interaction between Z_{eq} and Y_{eq}*

If the system instability is caused by the interaction between Z_{eq} and Y_{eq}, the product of Z_{eq} and Y_{eq} is the key factor according to the second step in the proposed criterion. Stability can be improved by decreasing the modulus of Z_{eq} or Y_{eq}; thus, the trajectory of $Z_{eq}\cdot Y_{eq}$ may avoid encircling the critical point (-1, 0) in the clockwise direction as shown in Fig. 13.

The equivalent Z module and equivalent Y module become more ideal because Z_{eq} or Y_{eq} is decreased. The most ideal examples are ideal voltage source (Z_{eq}=0) and ideal current source (Y_{eq}=0). The interaction between Z_{eq} and Y_{eq} also decreases no matter which variable is decreased; thus, the stability of the total system is enhanced. Z_{eq} and Y_{eq} can be reduced by decreasing the impedance or admittance of any sub-module or by adding a bus conditioner. The detailed methods remain related to the detailed model of each sub-module; however, this point is not emphasized in this study.

VI. Experimental Results

An experimental platform is established to verify the proposed criterion. Three sub-modules are connected to form a basic multi-module system. The validities of the proposed criterion are tested in different systems with different combinations of source and load because the proposed criterion does not depend on the power flow direction in the theoretical analysis. Photos of the test bench and network analyzer are shown in Fig. 14.

A. *First Group*

The detailed configuration in the first group is shown in Fig. 15. Buck/boost topology is utilized in each sub-module.

According to the configuration, the total system can be divided into three sub-modules as shown in Fig. 16. The multi-module system consists of one Z-type module and two Y-type modules.

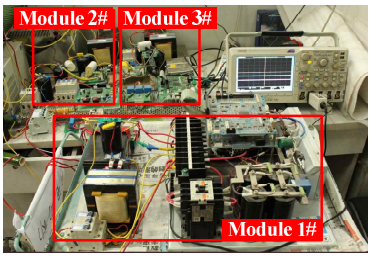

(a) Test bench.

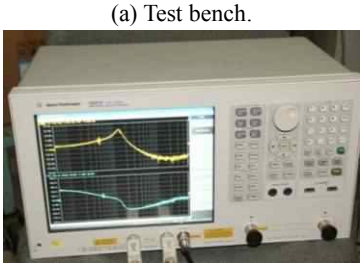

(b) Network analyzer.

Fig. 14. Experimental platform.

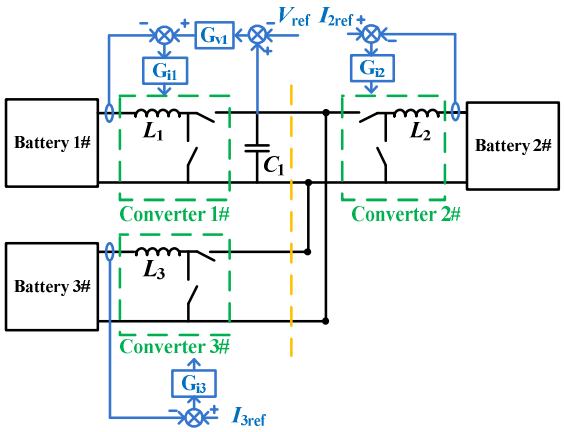

Fig. 15. Multi-module system in the first group.

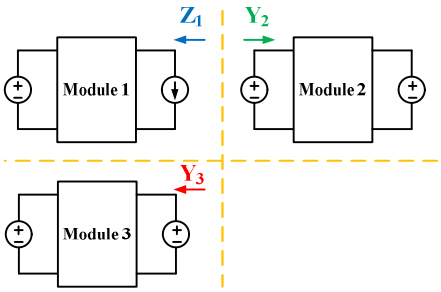

Fig. 16. Equivalent sub-modules in the first group.

The parameters in the first group experiment are shown in Table I. The input current of each battery is positive.

According to the system configuration, the system can be regarded as the combination of one voltage source with two current loads.

The module can also be stable in some cases even if only one RHP exists in the open-loop regulator. This condition can be easily explained by the Nyquist stability criterion.

1) *Stable case:* The detailed information of the terminal characteristics of each module is measured by Agilent

TABLE I

PARAMETERS IN THE FIRST GROUP

Reference Values	
V_{ref}	30 V
I_{2ref}	3.75 A
I_{3ref}	3.75 A
Output limit of voltage regulator (upper / lower)	15 / -15
Output limit of current regulator (upper / lower)	0.8 / 0.2
Circuit Elements	
C_1	1.5 mF
L_1, L_2, L_3	1 mH, 1 mH, 1 mH
Control Parameters in Stable Case	
Voltage Regulator in Module 1	1+40/s
Current Regulator in Module 1	0.1+40/s
Current Regulator in Module 2	1+40/s
Current Regulator in Module 3	1+40/s
Control Parameters in Unstable Case	
Voltage Regulator in Module 1	0.01+10/s
Current Regulator in Module 1	0.1+40/s
Current Regulator in Module 2	2*(s+200)/(s-200)
Current Regulator in Module 3	2*(s+200)/(s-200)

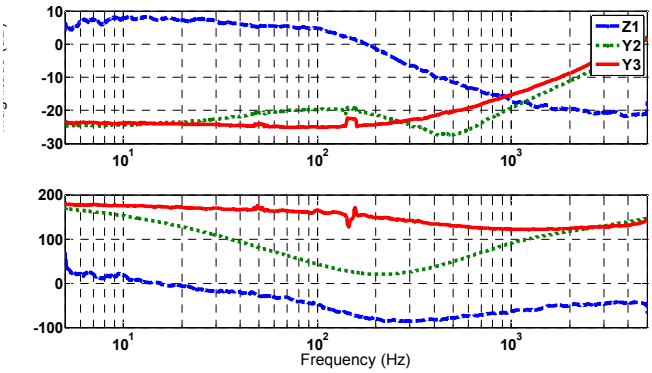

Fig. 17. Bode plots of the terminal characteristics of each module.

Network Analyzer E5061B. The measured data are redrawn in Matlab and shown in Fig. 17.

The proposed criterion is then applied to the measured data of each module. Given that only one Z-type module exists, only step 2 is required. T_m can be expressed as $Z_1 \cdot (Y_2+Y_3)$. The trajectory on the s-plane is drawn in Matlab based on the measured data and shown in Fig. 18.

No encirclement is observed around critical point (-1, 0). Therefore, the system is stable. All the three modules are connected, and the time domain waveforms are shown in Fig. 19. The system is stable as predicted.

2) *Unstable case:* The validity of the proposed criterion in the unstable case is also tested. Similar procedures are performed. The measured data of the terminal characteristics of each module are drawn in Fig. 20.

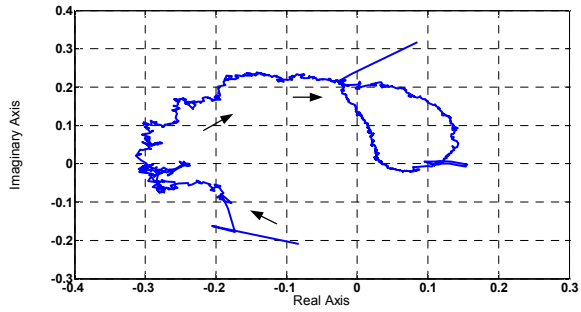

Fig. 18. Trajectory of $Z_1 \cdot (Y_2+Y_3)$.

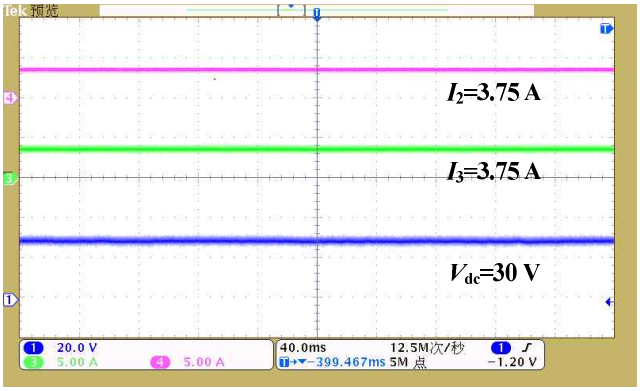

Fig. 19. Time domain waveforms of the multi-module system.

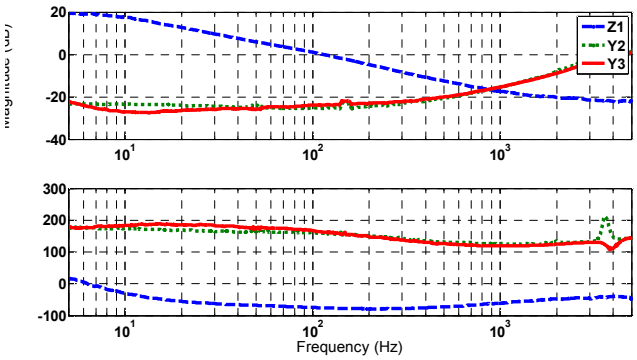

Fig. 20. Bode plots of the terminal characteristics of each module.

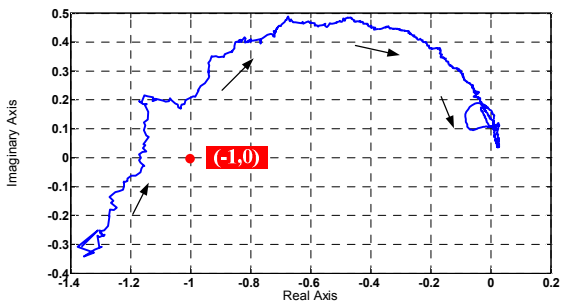

Fig. 21. Trajectory of $Z_1 \cdot (Y_2+Y_3)$.

The trajectory of $Z_1 \cdot (Y_2+Y_3)$ is drawn in Fig. 21.

The trajectory encircles point (-1, 0) once in the clockwise direction. Hence, the system is unstable according to the explanation of the proposed stability criterion. The time domain waveforms of the multi-module system are captured

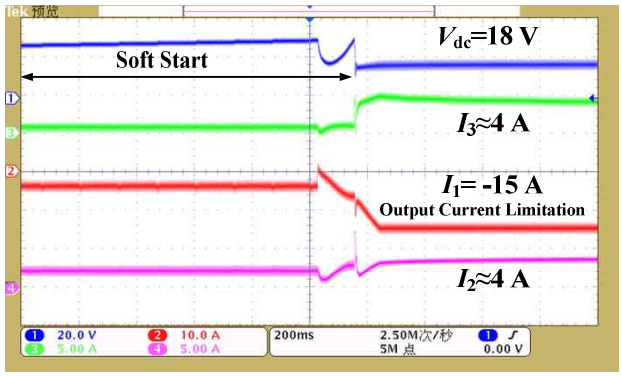

Fig. 22. Time domain waveforms of the multi-module system.

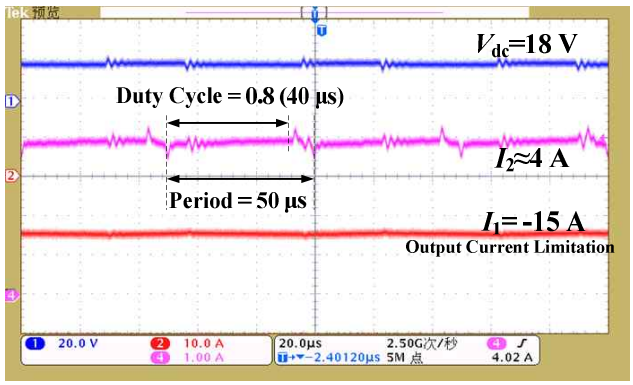

Fig. 23. Enlargement of Fig. 22.

in Figs. 22 and 23 to verify the stability assessment.

As shown in Fig. 22, the system shifts to another state after a soft start. The enlarged waveforms in Fig. 23 indicate that the outputs of the voltage regulator in module 1 and the current regulator in module 2 are saturated.

The system is unstable at the designed operating point. This result is consistent with that of the stability assessment. Therefore, the proposed criterion is valid in both stable and unstable cases in the first group.

The modulus of Z_1 in the stable case is much smaller than that in the unstable case. Therefore, the interaction between Z_{eq} and Y_{eq} decreases in the stable case, and system stability is improved.

B. Second Group

The detailed system structure in the second group is similar to that in the first group (Fig. 15). However, the reference values are changed to form a new system.

The parameters in the second group experiment are shown in Table II. The positive direction of each current is also defined as the input current of each battery.

According to the system configuration, the system can be regarded as the combination of one voltage source, one current source, and one current load. This setup is different from that in the first group. However, only the reference values are changed; the types of terminal characteristics of each module remain the same as those in the first group. The

TABLE II
PARAMETERS IN THE SECOND GROUP

Reference Values	
V_{ref}	30 V
I_{2ref}	7.5 A
I_{3ref}	-3.75 A
Circuit Elements	
C_1	1.5 mF
L_1, L_2, L_3	1 mH, 1 mH, 1 mH
Control Parameters in Stable Case	
Voltage Regulator in Module 1	1+40/s
Current Regulator in Module 1	0.1+40/s
Current Regulator in Module 2	1+40/s
Current Regulator in Module 3	1+40/s
Control Parameters in Unstable Case	
Voltage Regulator in Module 1	0.01+200/s
Current Regulator in Module 1	0.1+40/s
Current Regulator in Module 2	2*(s+200)/(s-200)
Current Regulator in Module 3	2*(s+200)/(s-200)

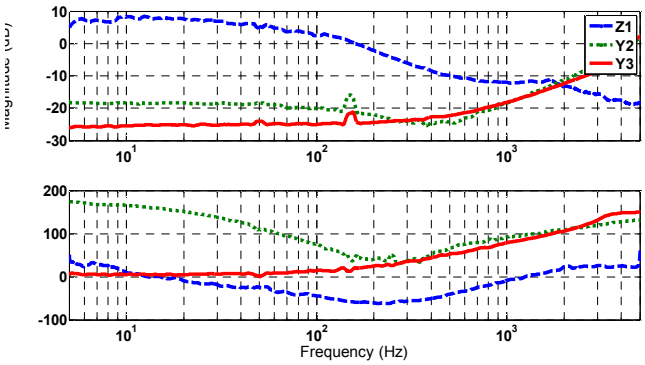

Fig. 24. Bode plots of the terminal characteristics of each module.

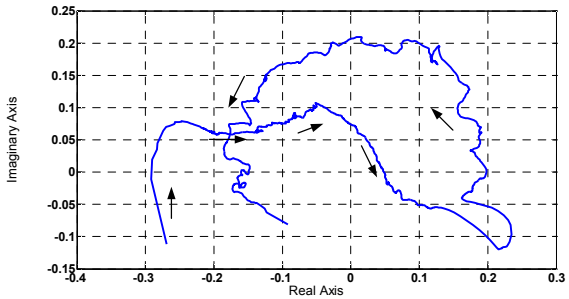

Fig. 25. Trajectory of $Z_1 \cdot (Y_2+Y_3)$.

system consists of one Z module and two Y modules.

1) Stable case: The measured data of the terminal characteristics of each module are drawn in Matlab and shown in Fig. 24.

The proposed criterion is then applied to the measured data of each module. T_m can be expressed as $Z_1 \cdot (Y_2+Y_3)$ although the system configuration is changed. The trajectory on the s-plane is drawn based on the measured data and shown in Fig. 25.

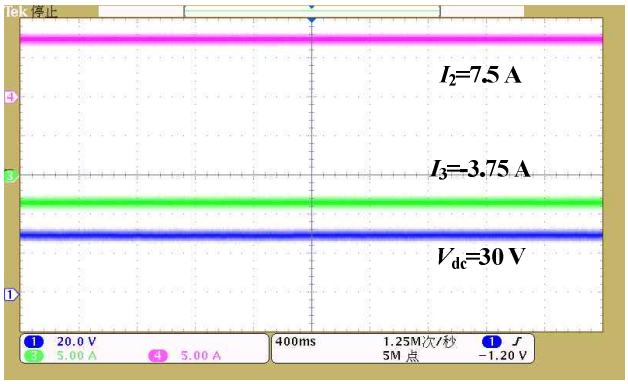

Fig. 26. Time domain waveforms of the multi-module system.

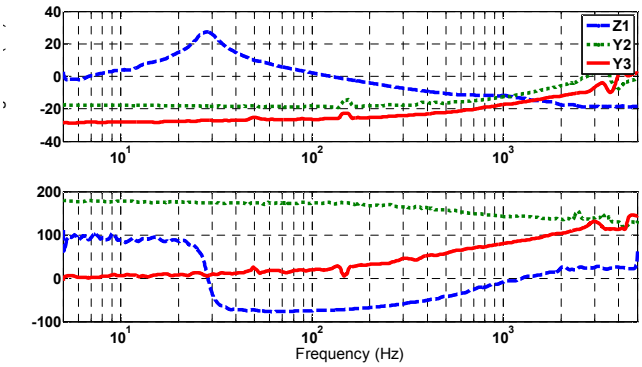

Fig. 27. Bode plots of the terminal characteristics of each module.

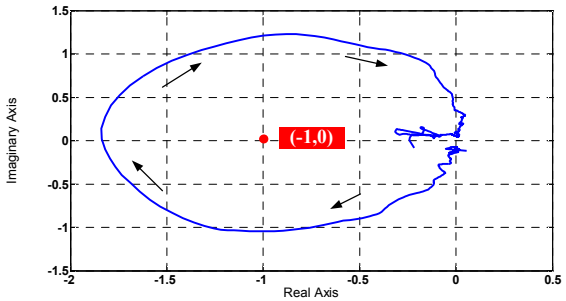

Fig. 28. Trajectory of $Z_1 \cdot (Y_2+Y_3)$.

No encirclement is found around point (-1, 0). Therefore, the system is stable. The time domain waveforms of the total system are shown in Fig. 26. The system is stable as predicted.

2) Unstable case: The validity of the proposed criterion in the unstable case in the second group is also tested. Similar procedures are implemented. The measured data of the terminal characteristics of each module are drawn in Fig. 27.

The trajectory of $Z_1 \cdot (Y_2+Y_3)$ is drawn in Fig. 28.

The trajectory encircles point (-1, 0) once in the clockwise direction. Hence, the system is unstable according to the proposed stability criterion. The time domain waveforms of the multi-module system are shown in Fig. 29.

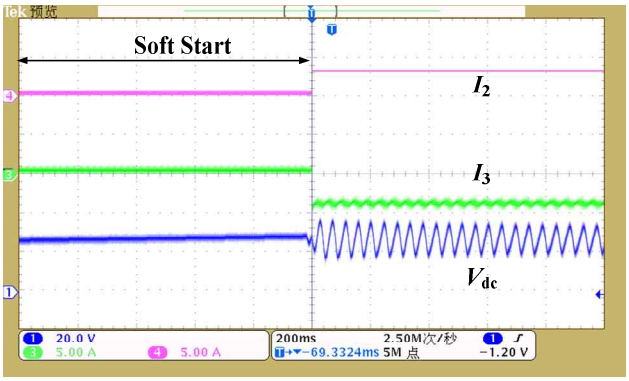

Fig. 29. Time domain waveforms of the multi-module system

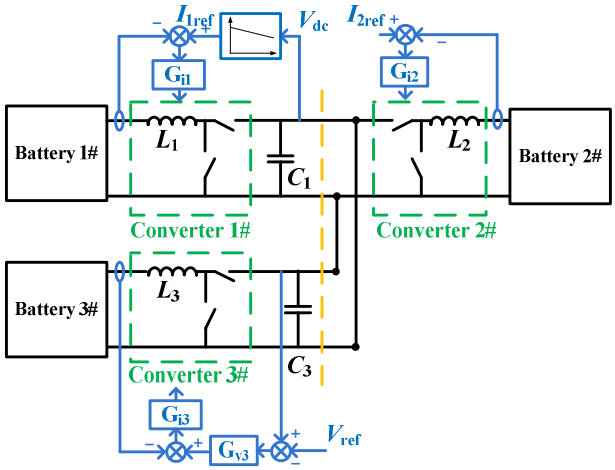

Fig. 30. Multi-module system in the third group.

The system becomes unstable after the soft start. Obvious oscillations can be observed in the DC bus voltage and the current of battery #3. Therefore, the proposed criterion is valid in both stable and unstable cases in the second group.

C. Third Group

In the first and second groups, only one Z-type module is utilized; thus, step 1 in the proposed criterion is neglected, and only the validity of step 2 is verified. The system is changed to test the validity of step 1, and the detailed structure is shown in Fig. 30. The system can be regarded as the combination of two voltage sources with one current load. Droop control strategy is adopted in module 1 to realize the parallel connection of two voltage sources without CSL.

The proposed stability criterion is suitable for the multi-module system without CSL. However, a current sharing strategy is still necessary when several sub-modules are used to maintain the DC bus voltage. Otherwise, the operating points of these converters would not be fixed if no natural current sharing strategy is used. Therefore, the proposed stability criterion will fail because there is no appropriate operating point to measure the small signal terminal characteristics. The most typical natural current sharing strategy without CSL is the droop method [28], [29].

Although the implementation of droop control affects the detailed model of the converter, the distinction between the terminal response and disturbance remains unchanged. Therefore, the type of terminal characteristics and the suitable stability criterion remain the same.

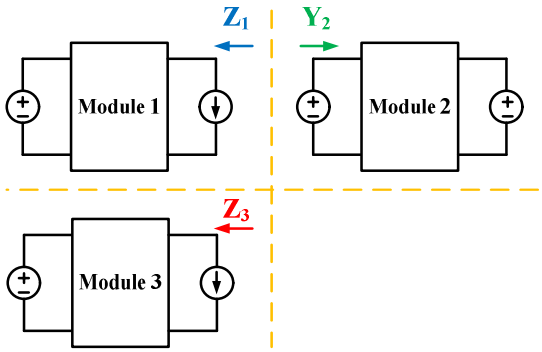

Fig. 31. Equivalent sub-modules in the third group.

TABLE III
PARAMETERS IN THE THIRD GROUP

Reference Values	
V_{ref}	30 V
I_{2ref}	7.5 A
Circuit Elements	
C_1, C_3	1.5 mF, 3.3 mF
L_1, L_2, L_3	1 mH, 1 mH, 1 mH
Control Parameters in Stable Case	
Voltage Droop Gain in Module 1	1
Current Regulator in Module 1	0.1+40/s
Voltage Regulator in Module 2	0.01+200/s
Current Regulator in Module 2	0.1+40/s
Current Regulator in Module 3	1+40/s
Control Parameters in Unstable Case	
Voltage Droop Gain in Module 1	2*(s+200)/(s-200)
Current Regulator in Module 1	0.1+40/s
Voltage Regulator in Module 2	0.01+200/s
Current Regulator in Module 2	0.1+40/s
Current Regulator in Module 3	1+40/s

According to the configuration, the total system can be divided into three individual modules as shown in Fig. 31. The multi-module system consists of two Z-type modules and one Y-type module. This setup is quite different from those of the first and second groups.

The parameters in the third group are shown in Table III.

1) *Stable case:* The measured data of the terminal characteristics of each module are shown in Fig. 32.

Given that two Z-type modules are used, the interaction between these two modules should be evaluated first. The trajectory of Z_1+Z_3 according to step 1 in the proposed criterion is drawn in Fig. 33.

The trajectory is located in the right half plane; thus, no encirclement is observed around point (0, 0), and the number of RHP in $Z_1||Z_3$ is 0.

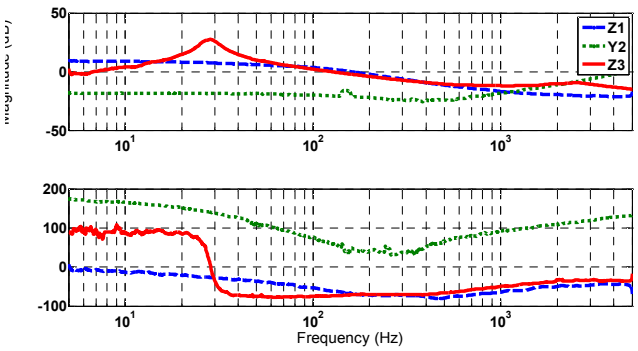

Fig. 32. Bode plots of the terminal characteristics of each module.

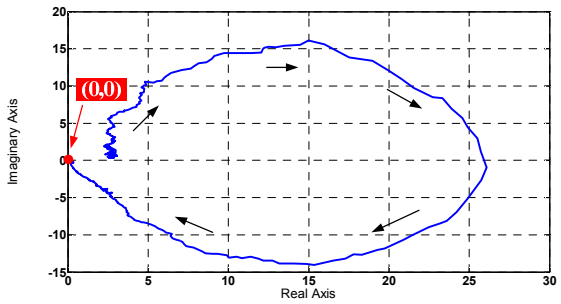

Fig. 33. Trajectory of Z_1+Z_3.

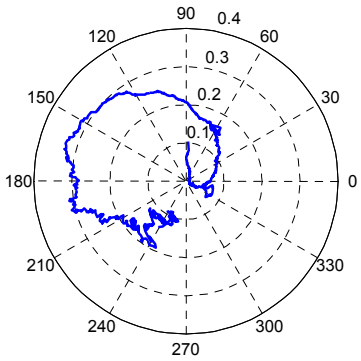

Fig. 34. Trajectory of $(Z_1\|Z_3)\cdot Y_2$.

Step 2 of the proposed criterion is then implemented. T_m can be expressed as $(Z_1\|Z_3)\cdot Y_2$, and the trajectory is drawn in Fig. 34.

No encirclement is found around point (-1, 0). The number of encirclements in step 2 is equal to that in step 1. Therefore, the system is stable. All the three modules are then connected, and the time domain waveforms are shown in Fig. 35. The stable status of the total system is consistent with the assessment of the proposed criterion.

2) *Unstable case:* Lastly, the validity of the proposed criterion in the unstable case in the third group is tested. Similar procedures are performed. The measured data of the terminal characteristics of each module are drawn in Fig. 36.

The trajectory of Z_1+Z_3 is drawn in Fig. 37. The trajectory encircles point (0, 0) once in the clockwise direction, and the number of RHP in $Z_1\|Z_3$ is 1.

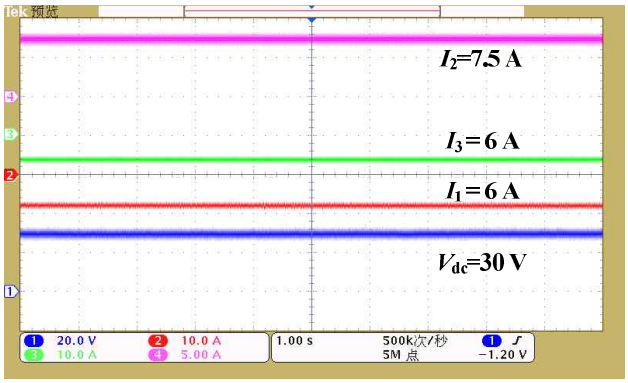

Fig. 35. Time domain waveforms of the multi-module system.

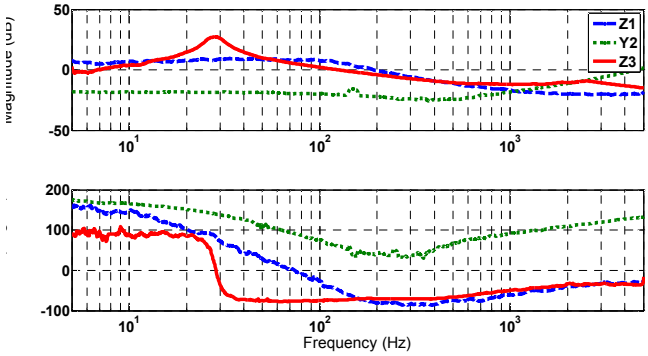

Fig. 36. Bode plots of the terminal characteristics of each module.

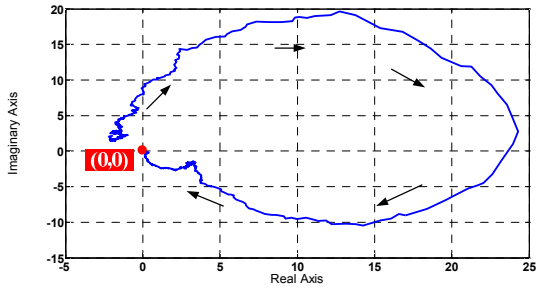

Fig. 37. Trajectory of Z_1+Z_3.

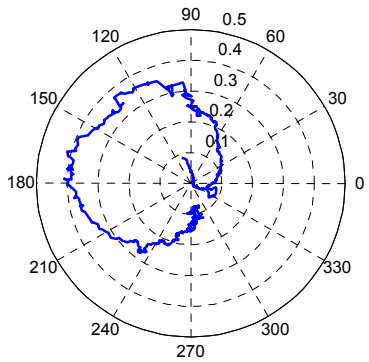

Fig. 38. Trajectory of $(Z_1\|Z_3)\cdot Y_2$.

The trajectory of $(Z_1\|Z_3)\cdot Y_2$ is drawn in Fig. 38.

No encirclement is observed around point (-1, 0). Thus, the number of encirclements in step 2 is not equal to that in step 1. Therefore, the system is unstable. All the three modules are

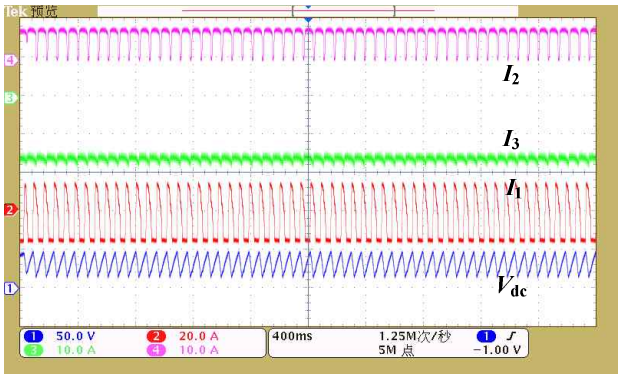

Fig. 39. Time domain waveforms of the multi-module system.

then connected, and the time domain waveforms are shown in Fig. 39.

The time domain waveforms are identical to those in the assessment of the proposed criterion. Therefore, the proposed criterion is valid in the stable and unstable cases in the third group.

VII. CONCLUSIONS

A generalized stability criterion for the multi-module distributed system without CSL was proposed. The different terminal characteristics of a sub-module were explained. The primary aim of this study is to assess stability based on the terminal behavior of each module rather than its function as a source or load. This method can be applied to different combinations of source and load modules. The experiment results verified the validity of the proposed criterion.

Theoretically, the proposed stability criterion is a sufficient and necessary condition for the stability assessment of multi-module distributed systems without CSL. However, some potential problems in practical application exist because of non-ideality. The measuring range and resolution of the network analyzer affect the accuracy of the measurement. The noise in the measurement also affects accuracy. These practical problems may lead to incorrect stability assessment when the trajectory is very close to the critical point such that whether the trajectory encircles the critical point or not is difficult to determine. In the study of the stability of cascade systems, this problem is solved by setting different forbidden regions to keep the trajectory off the critical point. Future work should focus on the design of forbidden regions in multi-module applications based on the proposed stability criterion as well as the design of sub-module control.

ACKNOWLEDGEMENTS

This work was supported in part by the National Basic Research Program (973 Program) of China under Project 2009CB219705 and in part by the State Key Laboratory of Electrical Insulation and Power Equipment under Project EIPE09109.

REFERENCES

[1] Y. Panov, J. Rajagopalan, and F. C.Lee, "Analysis and design of N paralleled DC-DC converters with master-slave current-sharing control," *Applied Power Electronics Conference and Exposition, 1997. Twelfth Annual*, Vol. 1, pp.436-442, Feb. 1997.

[2] X. Xie, S. Yuan, J. Zhang, and Z. Qian, "Analysis and Design of N paralleled DC/DC Modules with Current-Sharing Control," *Power Electronics Specialists Conference, 2006. PESC '06. 37th IEEE* , pp. 1-4, Jun. 2006.

[3] V. J. Thottuvelil and G. C. Verghese, "Analysis and control design of paralleled DC/DC converters with current sharing," *IEEE Trans. Power Electron*, Vol. 13, No. 4, pp.635-644, Jul. 1998.

[4] D. Hou, J. Liu, H. Wang, and W. Huang, "The stability analysis and determination of multi-module distributed power electronic systems," *Power Electronics for Distributed Generation Systems (PEDG), 2010 2nd IEEE International Symposium on*, pp.577-583, Jun. 2010.

[5] R. D. Middlebrook, "Design techniques for preventing input-filter oscillations in switched-mode regulators," *in Proc. Powercon 5*, pp. A3-1–A3-16, 1978.

[6] T. Suntio, J. Leppaaho, J. Huusari, and L. Nousiainen, "Issues on solar-generator interfacing with current-fed MPP-tracking converters," *IEEE Trans. Power Electron*, Vol. 25, No. 9, pp.2409-2419, Sep. 2010.

[7] J. Sun, "Impedance-based stability criterion for grid-connected inverters," *IEEE Trans. Power Electron,* Vol. 26, No. 11, pp.3075-3078, Nov. 2011.

[8] F. Liu, J. Liu, B. Zhang, H. Zhang, S. U. Hasan, and S. Zhou, "Unified stability criterion of bidirectional power flow cascade system," *Applied Power Electronics Conference and Exposition, 2013. Twenty-Eighth Annual IEEE*, pp.2618-2623, Mar. 2013.

[9] H. Wang, J. Liu, and W. Huang, "Stability prediction based on individual impedance measurement for distributed DC power systems," *Power Electronics and ECCE Asia (ICPE & ECCE), 2011 IEEE 8th International Conference on*, pp.2114-2120, May./Jun. 2011.

[10] T. Suntio, *Dynamic Profile of Switched-Mode Converter: Modeling, Analysis and Control*, Wiley Publications, 2009.

[11] M. Driels, *Linear Control Systems Engineering*, Tsinghua University Press, 2000.

[12] R. W. Erickson and D. Maksimovic, *Fundamentals of Power Electronics*, 2nd edition. New York: Kluwer, 2001.

[13] R. D. Middlebrook and S. Cuk. "A general unified approach to modelling switching-converter power stages," *In Power Electronics Specialists Conference,* Vol. 1, pp. 18-34. Jun. 1976.

[14] A. Capel, J. C. Marpinard, J. Jalade, and M. Valentin, "Current fed and voltage fed switching DC/DC converters - steady state and dynamic models their applications in space technology," *Telecommunications Energy Conference, 1983. INTELEC '83. Fifth International*, pp.421-430, 1983.

[15] D. Marx, P. Magne, B. Nahid-Mobarakeh, S. Pierfederici, and B. Davat, "Large signal stability analysis tools in dc power systems with constant power loads and variable power loads—A review," *IEEE Trans. Power Electron*, Vol. 27, No. 4, pp.1773-1787, Apr. 2012.

[16] W. Du, J. Zhang, Y. Zhang, and Z. Qian, "Stability criterion for cascaded system with constant power load," *IEEE Trans. Power Electron*, Vol. 28, No. 4, pp.1843-1851, Apr. 2013.

[17] E. Deng, "I. Negative Incremental Impedance of Fluorescent Lamps II. Simple High Power Factor Lamp Ballasts", *PhD thesis*, California Institute of Technology, Pasadena, California, 1996.
[18] E. Deng and S. Cuk, "Negative incremental impedance and stability of fluorescent lamps," *Applied Power Electronics Conference and Exposition, 1997. Twelfth Annual*, Vol. 2, pp.1050-1056, 1997.
[19] Y. Panov and M. Jovanovic, "Practical issues of input/output impedance measurements in switching power supplies and application of measured data to stability analysis," *Applied Power Electronics Conference and Exposition, 2005. Twentieth Annual IEEE,* Vol. 2, pp.1339-1345, Mar. 2005.
[20] M. Liu, H. Yuan, Y. Sun, and C. Yang, "Research on measurement of DC power supply impedance," *Electronic Measurement & Instruments, 2009. ICEMI '09. 9th International Conference on,* pp.2-703,2-706, Aug. 2009.
[21] R. Ridley, "Measuring frequency response: tips and methods," *Switching Power Magazine*, Vol. 3, No. 2, pp. 12-27, Spring 2002.
[22] C. K. Alexander and M. N. O. Sadiku, *Fundamentals of Electric Circuits*, McGraw-Hill Higher Education. 2005.
[23] F. Liu, J. Liu, B. Zhang, H. Zhang, and S. U. Hasan, "General impedance/admittance stability criterion for cascade system," *ECCE Asia Downunder (ECCE Asia), 2013 IEEE*, pp.422-428, 2013.
[24] K. Xing, J. Guo, W. Huang, D. Peng, F. C. Lee, and D. Borojevic, "An active bus conditioner for a distributed power system," *Power Electronics Specialists Conference, 1999. PESC 99. 30th Annual IEEE*, Vol. 2, pp.895-900, 1999.
[25] R. Ahmadi, D. Paschedag, and M. Ferdowsi, "Closed-loop input and output impedances of DC-DC switching converters operating in voltage and current mode control," *IECON 2010 - 36th Annual Conference on IEEE Industrial Electronics Society*, pp.2311-2316, 2010.
[26] M. K. Kazimierceuk, R. C. Cravens, and J. P. Harrington, "Closed-loop input impedance of a voltage-mode-controlled PWM boost DC-DC converter for CCM," *Circuits and Systems, 1994., Proceedings of the 37th Midwest Symposium on* , Vol. 2, pp.1253-1256, 1994.
[27] D. Kim, D. Son, and B. Choi, "Input impedance analysis of PWM DC-to-DC converters," *Applied Power Electronics Conference and Exposition, 2006. Twenty-First Annual IEEE*, pp. 1339-1346, 2006.
[28] B. T. Irving and M. M. Jovanovic, "Analysis, design, and performance evaluation of droop current-sharing method," *Applied Power Electronics Conference and Exposition, 2000. Fifteenth Annual IEEE*, Vol. 1, pp.235-241, 2000.
[29] J. W. Kim, H. S. Choi, and B. H. Cho, "A novel droop method for converter parallel operation," *IEEE Trans. Power Electron*, Vol. 17, No. 1, pp. 25-32, Jan. 2002.

Fangcheng Liu was born in China. He received his B.S. degree from Huazhong University of Science and Technology, Wuhan, China, in 2007. He is working for his Ph.D. in electrical engineering in Xi'an Jiaotong University. His current research interests include the modeling and control of hybrid energy storage systems and stability issues of multi-module systems.

Jinjun Liu was born in China. He received his B.S. and Ph.D. degrees in electrical engineering from Xi'an Jiaotong University (XJTU), China, in 1992 and 1997, respectively. He then joined the teaching faculty of XJTU Electrical Engineering School. In 1998, he led the founding of the XJTU/Rockwell Automation Laboratory and served as the laboratory director. From 1999 until early 2002, he served as a visiting scholar in the Center for Power Electronics Systems at Virginia Polytechnic Institute and State University, USA. He then came back to XJTU and in late 2002 was promoted to Full Professor and became the head of the Power Electronics and Renewable Energy Center at XJTU. From 2005 to early 2010, he served as the Associate Dean of the School of Electrical Engineering at XJTU. He is currently the Dean of Undergraduate Education at XJTU. He has co-authored three books, published over 100 technical papers, holds 13 patents, and received several national, provincial, and ministerial awards for scientific and career achievements, including the 2006 Delta Scholar Award. His research interests include power quality control, renewable energy generation and utility applications of power electronics, and modeling and control of power electronic systems. Dr. Liu is an AdCom member of the IEEE Power Electronics Society and serves as the China Liaison. He is also an Associate Editor for IEEE TRANSACTIONS ON POWER ELECTRONICS. He is an AdCom member and the Chair of the Student Activities Committee for the IEEE Xi'an Section. He is on Board of China Electrotechnical Society (CES) and serving as a Vice President for CES Power Electronics Society. He is also the Vice President on International Affairs for China Power Supply Society.

Haodong Zhang was born in China. He received his B.S. degree in electrical engineering from Xi'an Jiaotong University, Xi'an, China, in 2011. He is currently pursuing his M.S. degree in electrical engineering in the same university. His current research interests include control of hybrid energy storage systems and distribution generation systems.

Danhong Xue was born in China. She received her B.S. degree in electrical engineering from Xi'an Jiaotong University, Xi'an, China, in 2013. She is currently pursuing her M.S. degree in electrical engineering in the same university. Her current research interests include power electronics and control, which include microgrids and the stability of distribution generation systems.